Building Up of the Liquid-Ordered Phase Formed by Sphingomyelin and Cholesterol

C. Chachaty,* D. Rainteau,* C. Tessier,* P. J. Quinn,† and C. Wolf*
*Universite Paris 6, INSERM U538, Paris 75012, France; and †Life Sciences, King's College London, SE1 9NH, UK

ABSTRACT The long-range and molecular orders and dynamics in codispersions of egg sphingomyelin-cholesterol have been investigated by synchrotron x-ray diffraction and electron spin resonance using phosphatidylcholine spin-labeled at several positions on the *sn*-2 chain. Mixtures containing 0, 17, 33, 41, 50 mol% cholesterol exhibited a single phase by x-ray diffraction methods. The temperature dependence of the *d*-spacing between 20 and 50°C is attenuated with increasing proportions of cholesterol, becoming invariant for cholesterol contents of 41 and 50 mol% on completion of the liquid-ordered phase. Electron spin resonance revealed two sites for 17 and 33 mol% cholesterol. One site is highly ordered and the other is less ordered than the fluid phase of pure sphingomyelin as shown by the molecular and the intramolecular order parameters reflecting the segmental motions of the probe. The two-sites exchange rate indicates a mean lifetime of the sites of ~0.1 μs during which the lipid displacement is ~1 nm. The short lifetime of the sites probed by ESR and the single phase detected by x-ray diffraction support in this binary mixture, the building up of the Lo phase by a progressive accumulation of randomly distributed sphingomyelin-cholesterol condensed complexes rather than by diffusional exchange between extended domains.

INTRODUCTION

The association of sphingomyelin (SM) and cholesterol (CHOL) in complex mixtures of membrane lipids is said to create domains of liquid-ordered phase (Lo) that phase separate from disordered fluid lamellar phase denoted Lα or Ld (Sankaram and Thompson, 1990). Condensed phases have also been reported in mixtures of cholesterol and saturated molecular species of glycerophospholipids leading to the suggestion that fluid phase immiscibility may create domains in biological membranes (Ipsen et al., 1987; Recktenwald and McConnell, 1981). More recently, interest has concentrated on the size and stability of domains that may be formed by phospholipid-cholesterol mixtures. Condensed complexes (McConnell and Vrljic, 2003) on the one hand, may form without detectable phase separation of recognizable lipid phases or they may separate into domains of stable stoichiometric complexes. Clearly, the tendency to form transient phase-separated domains would be a desirable characteristic in the execution of biochemical functions.

The ability to distinguish condensed complexes in a homogeneous phase from ''macroscopic'' phase-separated domains depends on the detection method. X-ray diffraction techniques rely on long-range ordering of the assembly of phospholipids and cholesterol molecules whereas spectroscopic methods are sensitive to short-range interactions. Spectroscopic methods as NMR and electron spin resonance (ESR) considered thereafter are sensitive to short-range interactions and appropriate to the measurement of the molecular order and dynamics. These methods also provide information on the intersite exchange within different and complementary timescales: from 1 μs to 10 ms for NMR, 0.01–1 μs for ESR using nitroxide spin probes. By means of spectral shape analysis, NMR is able to measure the exchange rate between sites separated by tens or hundreds of nanometers against a few nanometers for ESR spin probe. These considerations are relevant to the determination of the lateral extension of ordered and disordered domains in membranes or to the lifetime of these domains. Thus, condensed complexes that would form, so-called, nanodomains with lifetimes shorter than 1 μs fall conveniently into the range of X-band ESR spectroscopy.

Many studies of the phase behavior of phospholipid-cholesterol mixtures employ synthetic lipids comprised of a single fatty acyl composition. Phase diagrams showing coexistence of Lo and Lα phases in mixtures of cholesterol and phosphatidylcholines with disaturated (Almeida et al., 1992; Vist and Davis, 1990) and diunsaturated (Hagen and McConnell, 1997) fatty acyl chains have been reported.

Although single-molecular species exhibit well-characterized cooperative thermotropic phase behavior such mixtures cannot be considered as models of biological membranes that comprise a variety of molecular species with distinct transition temperature. A consensus is emerging from studies of phospholipid-cholesterol mixtures using a variety of biophysical methods that phase behavior and complex formation is highly dependent on the particular molecular species of phospholipid. As it will be shown later, the behavior of egg SM consisting of a number of different molecular species observed in this study, for example, differ appreciably from that seen in synthetic disaturated phospholipids such as dimyristoyl- and dipalmitoyl-phosphatidylcholines. This distinction cannot be entirely accounted for by differences in the structure of sphingo- and glycerophospholipids. The unusually long amide-linked fatty

Submitted October 7, 2004, and accepted for publication February 28, 2005.
Address reprint requests to Claude Wolf, E-mail: wolf@ccr.jussieu.fr.

0006-3495/05/06/4032/13 $2.00
doi: 10.1529/biophysj.104.054155

acids (C24:0 and C24:1) associated with SM of natural origin are believed to be responsible for their high affinity for cholesterol and tendency to phase separate from fluid phospholipids in bilayers (Calhoun and Shipley, 1979; Dietrich et al., 2001). Another particularity of these long acyl chain derivatives is their ability to interdigitate in the absence of cholesterol. Presently, dealing with a mixture of molecular species possessing different affinities for cholesterol, a segregation between cholesterol enriched and depleted domains can occur, resulting in short-range heterogeneities. The detection of such heterogeneities demands methods sensitive to short-range intermolecular interactions. Furthermore, because the dispersed complexes are likely to be metastable their detection requires observations within an appropriate timescale.

The application of static methods only such as x-ray diffraction and atomic force microscopy are unsatisfactory in resolving the phase separation. Thus, x-ray diffraction methods (Gandhavadi et al., 2002) indicate a single lamellar phase in a dispersion of equimolar dioleoylphosphatidylcholine/brain sphingomyelin/cholesterol, the archetypical membrane raft (Edidin, 2003), whereas atomic force microscopy of a mixture with only slight difference in the fatty acid composition (Rinia et al., 2001) shows the separation of two distinct phases.

We have addressed this question by combining two complementary approaches characterizing the molecular order and dynamics of mixed dispersions of cholesterol and egg SM, namely, synchrotron x-ray diffraction and ESR. Results will be interpreted in the light of NMR studies (Aussenac et al., 2003; Filippov et al., 2003; Guo et al., 2002; Huang et al., 1993; Vist and Davis, 1990) because they complement ESR with a distinct timescale. In the whole range of cholesterol concentration explored, the diffraction studies show a single lamellar phase with no evidence of a separation of extended domains. For cholesterol contents below 40%, however, ESR reveals two distinct environments of the probe that can be clearly distinguished by molecular ordering and mobility. The rate of exchange between the sites and their lifetimes have been determined by spectral simulation as a function of temperature and cholesterol concentration. A simulation procedure has been applied that discriminates between the overall reorientational motion and the segmental mobility of the *sn*-2 chain supporting the spin-label reporter group. When the proportion of cholesterol exceeds 40 mol% a single site is observed by ESR that signifies the creation of a continuous liquid-ordered phase. Simultaneously the temperature-independent behavior of the phase suggests a conversion of the liquid-disordered phase into the compact liquid-ordered phase. This is observed in the egg sphingomyelin mixture comprised of different molecular species of lipid in which there is no clear distinction between cholesterol-rich and cholesterol-depleted domains. Finally, the data are consistent with a heterogeneous model represented by the emergence of a liquid-ordered phase from a progressive collapse of metastable domains that are comprised of more and less ordered nanodomains, into a homogeneous Lo phase.

MATERIAL AND METHODS

Materials

Lipids (SM, CHOL) were purchased from Sigma (Sigma-Aldrich, St. Quentin-Fallavier, France). The fatty acid composition of SM was examined by gas chromatography/mass spectrometry to confirm the absence of degradation products after exposure to the synchrotron x-ray beam. Egg sphingomyelin is mostly amidified with C16:0 (68%) and C18:0 (16%) but also contains a proportion of very long-chain fatty acids (C22:0, 5%; C24:0, 2%; and C24:1, 1%). The presence of these unusually long fatty acids is important for model mixtures in the context of membrane rafts as they are abundant in detergent-resistant fractions from biological membranes (Koumanov et al., 2005).

XRD measurements

Samples for x-ray diffraction (XRD) examination were prepared by dissolving lipids in chloroform/methanol (2:1, vol/vol) and mixing in the desired proportions denoted as mol% relative to the total mol of lipid. The organic solvent was subsequently evaporated under a stream of oxygen-free dry nitrogen at 45°C and any remaining traces of solvent were removed by a storage under high vacuum for two days at 20°C. The dry lipids were hydrated with an equal weight of 100 mM Tris-HCl (pH 7.5) buffer according to the following protocol: the lipid dispersion was thoroughly stirred with a thin needle, sealed under argon, and was annealed by 50 thermal cycles between 20 and 65°C. The samples were stored at 4°C before examination. Mixing of the lipids was consistent with the absence of sharp reflections observed at *d*-spacings corresponding to 3.23 and 0.379 nm that arise from cholesterol microcrystallites in samples where lipid phase separation takes place.

X-ray diffraction measurements were performed at station 16.2 of the Daresbury Synchrotron Radiation Source (Cheshire, UK). Simultaneous small-angle (SAXS) and wide-angle (WAXS) x-ray scattering intensities were recorded so that a correlation could be established between the mesophase repeat spacings and the packing arrangement of acyl chains. The SAXS quadrant detector response was corrected for channel response using a static radioactive iron source (sample to detector distance, 2 or 2.5 m) and calibrated for *d*-spacings using hydrated rat-tail collagen. The WAXS intensity profiles were measured with a curved INEL detector (Instrumentation Electronique, Artenay, France) that was calibrated using the diffraction peaks from high-density polyethylene. The lipid dispersion sample (20 μl) was sandwiched between two thin mica windows 0.5-mm apart and the measurement cell was mounted on a programmable temperature stage (Linkam, Surrey, UK). The temperature was monitored by a thermocouple (Quad Service, Poissy, France) inserted directly into the lipid dispersion. The setup, calibration, and facilities available on the station 16.2 Web site are described in http://www.srs.dl.ac.uk/ncd/station82/description.html. Data reduction and analysis were performed using the OTOKO for a personal computer program kindly provided by M. H. J. Koch (Boulin et al., 1986).

ESR measurements

To obtain an estimate of the ordering and flexibility of pure SM and SM-CHOL mixtures at different depths within the bilayer, phosphatidylcholine probes labeled with a doxyl radical at different positions of the *sn*-2 chain were used. Spin-labeled PC (1-palmitoyl-2-stearoyl(*n*-doxyl)-*sn*-glycero-3-phosphocholine where $n = 5, 7, 10, 12, 14, 16$, denoted hereafter, PC-*n*)

were purchased from Avanti Polar Lipids (Alabaster, AL) and were added to lipid mixtures in chloroform/methanol (2:1, vol/vol). Preliminary experiments were performed with a spin-probe concentration of 1 mol%. This concentration was subsequently reduced to 0.1 mol% without deterioration of the signal/noise ratio because of the line narrowing. After evaporation of the solvent the dry lipids were hydrated with a large excess of Tris-HCl buffer (400 μl, 10 mM, pH 7.5). The lipid dispersion was centrifuged and 20 μl of the pelleted liposomes were transferred to a capillary ESR measurement cell and sealed. Continuous wave ESR spectra were recorded at 9.5 GHz using a Bruker, ER 200D ESR spectrometer (Wissembourg, France) after an equilibration time (~5 min) at each temperature set by the variable temperature device (Bruker ER4111VT). The signal was digitized by EPRWARE software (Scientific Software Service, Bloomington, IL).

Analysis of ESR spectra

Accurate determination of order parameters and reorientation correlation times of spin probes was achieved by fitting simulated to experimental spectra. The simulations have been performed using an improved version of the LQCF program (Chachaty and Soulié, 1995; Chachaty and Wolf, 1999) and the NLSL program (Budil et al., 1996). Both programs utilize modified versions of the Levenberg-Marquardt's algorithm (Marquardt, 1963) with an automated least-squares fitting of experimental spectra for the optimization of ESR parameters. The order parameter of the probe is $S_{zz} = (1/2)\langle 3\cos^2\theta(t) - 1\rangle$, θ being the time-dependent angle between the z axis of magnetic tensors and the local director Δ_L. The average reorientation correlation time is $\bar{\tau} = (\tau_\perp^2 \tau_\parallel)^{1/3}$, $\tau_\perp$ and $\tau_\parallel$ corresponding to the tumbling of the z axis and to the rotation about it, respectively.

The subsidiary parameters for fitting spectra using LQCF and NLSL programs are the Gaussian inhomogeneous broadening, ΔH_G, and the Lorentzian linewidth, ΔH_L, dependent on the electron spin-spin interactions as well as the asymmetry of the ordering tensor $\eta = (S_{xx} - S_{yy})/S_{zz}$, which can be accurately determined by high field experiments (Kurad et al., 2004).

An example of spectrum showing the coexistence of two sites is shown in Fig. 1 *B* where it may be compared with single-component spectra (Fig. 1, *A* and *C*). The LQCF and NLSL programs are used to determine the relevant ESR parameters and proportion of each site. LQCF also provides an estimate of the exchange rate ν_{ex} between the two sites assuming that the orientation of the local director Δ_L remains unchanged (Davoust and Devaux, 1982; Marsh, 1989).

The LQCF program determines $\bar{\tau}$ under the fast motional regime ($\bar{\tau}$<2 ns) from the quadratic dependence of the homogeneous linewidth on the nuclear magnetic quantum number M_I using the general expression given in Nordio (1976) with spectral densities from Freed (1977). Under the slow motional regime S_{zz} and $\bar{\tau}$ are obtained from the NLSL program based on the stochastic Liouville equation (Schneider and Freed, 1989), which yields optimized values of the parameters up to 7–8 ns, the longest reorientation correlation time encountered in this study. Fig. 2 shows fittings obtained with these programs. The standard deviation between experimental and simulated spectra after optimization is expressed as percentage of the maximum amplitude of the experimental spectrum.

The dynamics of nitroxide groups attached to long-chain molecules has been a subject of sophisticated studies taking into account the overall reorientation of the probe as well as the segmental motions that have been applied to the simulation of spectra of spin-labeled phospholipids in oriented samples (Cassol et al., 1993, 1997; Lange et al., 1985; Moser et al., 1989). More recently, the contributions of overall reorientation of the probe and segmental motions have been estimated by ESR for randomly oriented samples at X-band frequency and at very high magnetic fields (Livshits et al., 2004; Lou et al., 2001). The reorientation correlation times given by NLSL or LQCF programs applied to flexible spin-labeled molecules are intricate functions of dynamic, conformational, and ordering parameters. To obtain an estimate of these parameters from the fittings of randomly oriented samples, we have written the DOXFIT program based on previous nuclear relaxation studies on flexible molecules (Caniparoli et al., 1988; Chachaty and Bredel, 1991; Chachaty and Langlet, 1985). The DOXFIT program applied to the fittings of spectra from PC-5 through PC-14 (Figs. 3 and 4) proceeds in three steps.

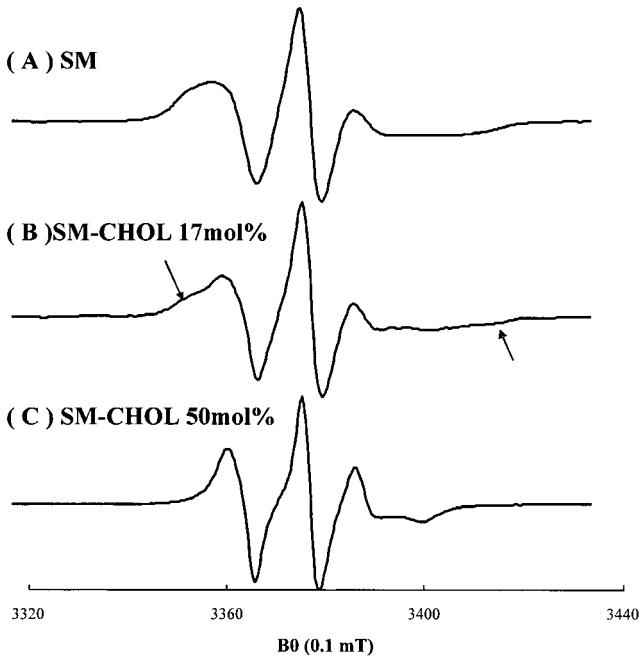

FIGURE 1 ESR spectra of the PC-16 spin probe recorded at 17°C. (*A*) Egg sphingomyelin (*SM*) without cholesterol, Lβ phase. The spectral fittings yield $S_{zz} = 0.4$, $\bar{\tau} = 2.2$ ns. (*B*) SM-CHOL 17 mol%. The outermost features indicated by arrows show the presence of two components. The fitting of the two-component spectrum yields $S_{zz} = 0.5$, $\bar{\tau} = 1.6$ ns for a site, and $S_{zz} = 0.3$, $\bar{\tau} = 3.6$ ns for the other site. (*C*) SM-CHOL 50 mol%, Lo phase. The spectral fittings yield $S_{zz} = 0.3$, $\bar{\tau} = 0.7$ ns.

Step 1: order parameters

As the doxyl radicals are attached to an alkyl chain, S_{zz} depends on the populations of *trans* and *gauche* rotamers about the C-C bonds (Hubbell and McConnell, 1971). It may be expressed as $S_{zz} = S_{mol}S_{tilt}S_C$. S_{mol} is the molecular order parameter, i.e., the order parameter of the longitudinal axis Δ_M of the molecular rotational diffusion tensor with respect to Δ_L, $S_{tilt} = (1/2)(3\cos^2\delta - 1)$ where δ is the angle between Δ_M and the mean axis Δ_C of the *sn*-2 chain, and S_C is the order parameter of the z axis of magnetic tensors with respect to Δ_C. S_C depends on the position of the doxyl group and is obtained by fitting the relative values of S_{zz} with values obtained with the LQCF program, taking as the adjustable parameters the populations P_T of the *trans* rotamer about the 13 bonds involved in the motion of doxyl groups up to position 14. Position 14 is the limit for the memory size of the personal computer allocated by our software. To reduce the number of adjustable parameters the bonds of the alkyl chain have been divided into four groups where P_T was taken constant: bond numbers 1–6, 7–9, 10 and 11, 12 and 13. For the absolute fitting of the observed values of S_{zz} along the chain, there are therefore five adjustable parameters including $S_{mol}S_{tilt}$, initially considered as a single parameter. S_{mol} and S_{tilt} have distinct influences on the linewidth and can be separately estimated in further steps of the calculation. In addition to S_{zz}, the procedure allows the calculation of the asymmetry parameter of the ordering tensor at all doxyl positions.

Assuming that *gauche*$^+$ (G^+) and *gauche*$^-$ (G^-) rotamers are energetically equivalent, there are potentially 3^{13} conformers between positions 1 and 14 of the *sn*-2 chain. This number is substantially reduced by

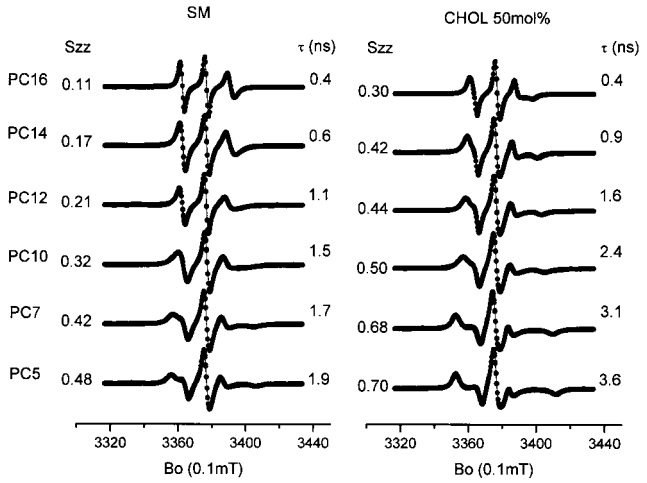

FIGURE 2 Experimental (*solid line*) and computed (*dots*) spectra of PC-5–16 probes in pure SM (*left panel*) and SM-CHOL 50 mol% (*right panel*) at 41°C. The fittings have been performed by means of the LQCF or NLSL programs with S_{zz} and $\bar{\tau}$ as the main adjustable parameters. For these fittings, we have taken $g_{xx} = 2.0091$, $g_{yy} = 2.0061$, $g_{zz} = 2.0022$ ($g_0 = 2.0058$) for the **g** tensor and $a_{xx} = a_{yy} = 0.516$mT, $a_{zz} = 3.3$mT ($a_N = 1.444$mT) for the hyperfine coupling tensor **A**. These principal values are means of values given in Ge et al. (1999) for the spin probes PC-5 and PC-16 in DPPC and SM. Owing to the local polarity, the hyperfine coupling constant a_N decreases from ~1.55 to ~1.4 mT from PC-5 to PC-16 and depends also on the CHOL concentration. The principal values of **A** have therefore been corrected by a factor $f_A = a_N/1.444$, which is adjusted in spectral fittings using the LQCF program.

removing the conformers containing the sterically unfavorable G^+G^- local form involving a folding back of the chain (Flory, 1969). To make the calculation procedure tractable with a PC, a further reduction is achieved by selecting the 300–1200 most probable conformers representing >90% of the

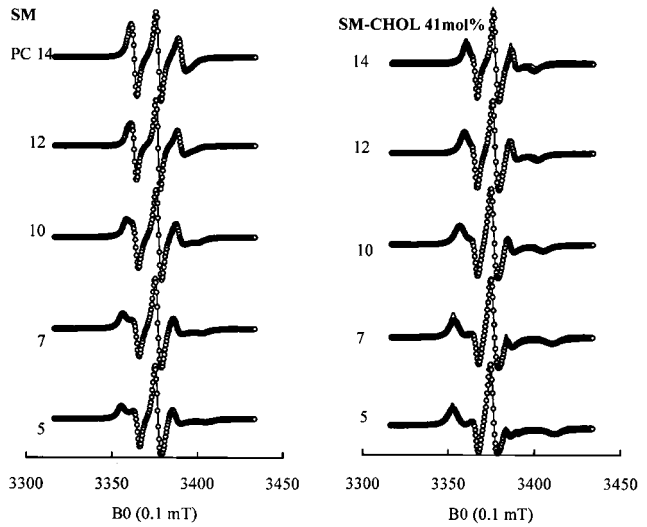

FIGURE 3 Experimental (*solid line*) and computed (*dots*) spectra of PC-5–14 spin probes in pure sphingomyelin (*left panel*) and SM-CHOL 41 mol% (*right panel*) samples at 41°C. The simulations have been performed using the DOXFIT program that takes into account the overall molecular as well as the segmental orderings and motions using the parameters given in Table 3.

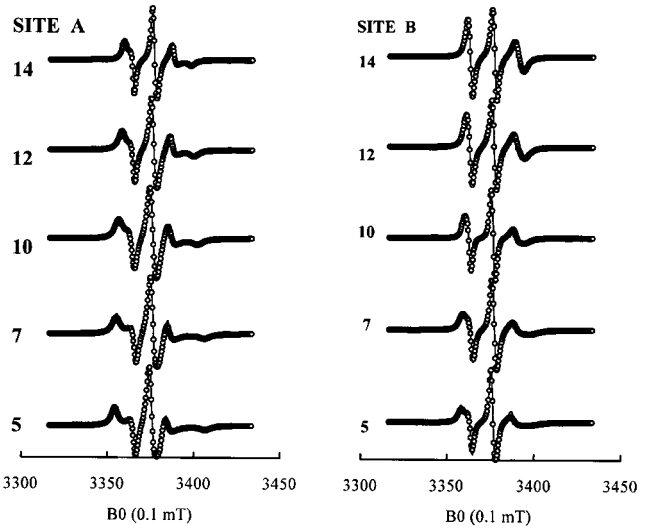

FIGURE 4 Fittings of the two spectral components of PC spin probes in the SM-CHOL 17 mol% sample at 41°C. The solid lines represent the component A (the most ordered site) and the component B simulated with parameters from the fitting of experimental spectra by means of the LQCF program. The dots correspond to the simulation of the A and B components by means of the DOXFIT program with parameters given in Table 3.

total conformer population. It was verified that this limitation in the number of conformers has no significant effect on the final results.

Step 2: linewidth

The homogeneous linewidths are computed for a quadratic dependence upon M_I (Nordio, 1976) with spectral densities adapted from Caniparoli et al. (1988) and Chachaty and Bredel (1991). These parameters depend on S_{mol} and S_C, on the reorientation correlation times $\tau_{\perp}^{M}$ and $\tau_{//}^{M}$ for the tumbling of the molecular axis Δ_M and for the rotation about it, as well as on the probability per unit time $W_{G\rightarrow T}$ of the *gauche* → *trans* transition kept invariant along the chain.

Step 3: spectral fittings

While in steps 1 and 2 the parameters are adjusted manually, the spectral fittings are automated, using a program similar to LQCF with S_{zz}, ΔH_G, and ΔH_L linewidths as adjustable parameters. If the optimized values of S_{zz} differ significantly from the values obtained in step 1, the parameters S_{mol}, δ, and P_T are revised and the whole process is restarted from step 1.

The accuracy of spectral fittings by means of the DOXFIT and LQCF programs are comparable with standard deviations in the range 0.5–1.5%.

More details on these programs, available on request, may be obtained from claude.chachaty@wanadoo.fr.

RESULTS

Synchrotron x-ray diffraction

The thermotropic phase behavior of egg sphingomyelin is complex reflecting the mixture of different molecular species. This behavior is modified by the presence of cholesterol in a manner that depends on the proportion present in the mixture. The structural features of the transitions observed in egg sphingomyelin are shown in Fig. 5 *A*. This shows a

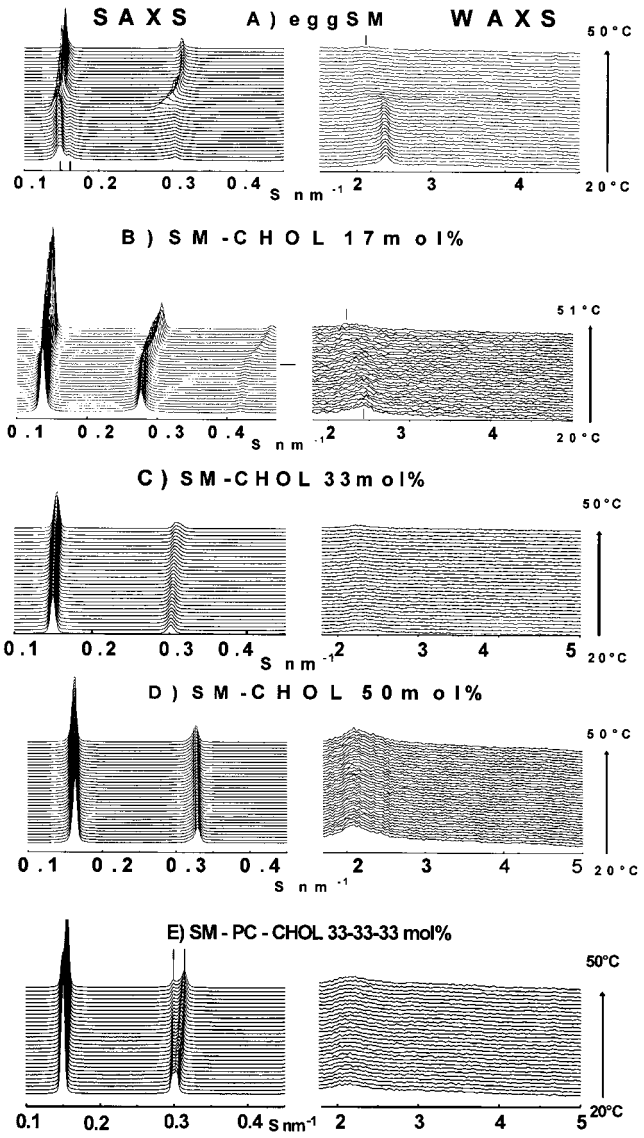

FIGURE 5 Small-angle (*SAXS*, *left panel*) and wide-angle (*WAXS*, *right panel*) x-ray scattering intensity recorded for multilamellar aqueous dispersions of egg SM mixed with increasing CHOL concentrations (*A*) egg SM; (*B*) SM-CHOL 17 mol%; (*C*) SM-33 mol%; (*D*) SM-CHOL 50%; (*E*) ternary mixture equimolar SM-PC-CHOL mixture. The sequence of diffractograms is recorded during the initial heating scan from 20 to 50°C (1 frame per °C, scan rate 1°C/min). Tick marks identify the values cited in Results for the reciprocal spacing (S, given in nm^{-1}) and temperature. Fig. 5 *E* (ternary equimolar mixture SM-PC-CHOL) shows the coexistence of two phases (tick marks).

sequence of SAXS/WAXS intensity profiles recorded during a heating scan from 20 to 50°C. During the scan of the sample that had been equilibrated before x-ray examination for >1 day at 4°C a lamellar gel ($L\beta$)-to-lamellar fluid ($L\alpha$) transition is detected with an onset temperature of 35°C and an end temperature of 44°C. The $L\beta$ phase is characterized by a lamellar repeat spacing of 6.75 nm and a sharp wide-angle *d*-spacing of 0.42 nm typical of hexagonally packed hydrocarbon chains in gel phase. A minor small-angle lamellar repeat is also observed with a *d*-spacing of 6.29 nm. This structure is assigned to an interdigitated lamellar gel phase designated $L\beta^*$. The interdigitated phase coexists with $L\beta$ phase at temperatures up to the onset of the gel to liquid-crystalline phase transition at 35°C. The interdigitated phase is firstly converted to noninterdigitated lamellar phase with a *d*-spacing of ~7.10 nm and the chains begin to undergo a transition to a liquid-crystal configuration evidenced by the broadening and shift of the WAXS peak to a spacing corresponding to 0.46 nm shown by the tick mark at 50°C. The disordering of the hydrocarbon chains is associated with a progressive decrease in *d*-spacing of the lamellar repeat that reaches a value of 6.34 nm at 50°C. The formation of $L\beta^*$ during equilibration of egg sphingomyelin at 4°C is believed to be due to the small proportion of molecular species with long amide-linked fatty acids (C22; C24) resulting in pronounced chain-length asymmetry (Boggs and Koshy, 1994).

Codispersions of egg sphingomyelin with 17 mol% cholesterol subjected to a similar heating scan (Fig. 5 *B*) show three peaks corresponding to the first three orders of diffraction of a single lamellar phase. At temperatures below ~36°C the *d*-spacing of the lamellar phase is 7.25 nm and the WAXS profile shows a broad peak centered at a spacing of 0.417 nm. There is a progressive shift in lamellar *d*-spacing with increasing temperature >38°C reaching a value of ~6.52 nm at 50°C. There is a corresponding broadening of the WAXS peak and a shift in the peak position to a *d*-spacing of 0.439 nm. The temperature range over which the transition takes place is significantly extended by the presence of 17 mol% cholesterol and there is no evidence for formation of an interdigitated phase. Equilibration of sphingomyelin-cholesterol dispersions at 4°C for prolonged periods did not result in the appearance of interdigitated lamellar phase.

The effect of cholesterol on the temperature dependence of the phase transition of egg sphingomyelin is shown in Fig. 6 where lamellar *d*-spacings are plotted as a function of temperature during an initial heating and subsequent cooling scan between 20 and 50°C. The hysteresis in the phase transition of the pure phospholipid is clearly evident in Fig. 6 *A* and is eliminated by the presence of 17 mol% cholesterol (Fig. 6 *B*). With increasing proportions of cholesterol in the sphingomyelin bilayers the temperature-dependent changes in lamellar *d*-spacing are reduced (Fig. 6, *C–E*). Similar *d*-spacings have been reported for codispersions of bovine brain sphingomyelin dispersed with cholesterol (Gandhavadi et al., 2002). Furthermore there is no evidence for any phase separation within the mixtures (Fig. 5, *B–D*).

The apparent homogeneous mixing of sphingomyelin and cholesterol over molar proportions ranging up to equimolar is in marked contrast to ternary mixtures containing egg phosphatidylcholine. This is exemplified in Fig. 5 *E*, which shows a sequence of SAXS/WAXS patterns recorded

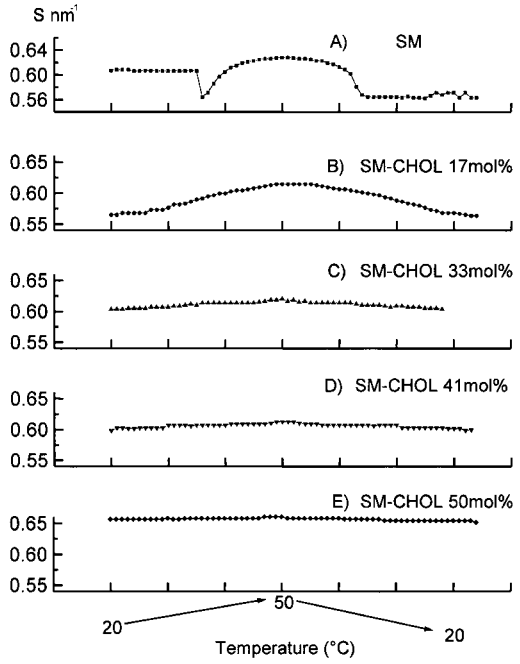

FIGURE 6 Variation as a function of the temperature of the *d*-spacing of the lamellar phase identified by SAXS in multilamellar aqueous dispersion of SM-CHOL mixtures. For each concentration (*A*, egg SM; *B*, SM-CHOL 17 mol%; *C*, SM-CHOL 33 mol%; *D*, SM-CHOL 41 mol%; and *E*, SM-CHOL 50 mol%) the reciprocal *d*-spacing (S in nm^{-1}) is plotted as a function of the temperature at the rate of ± 1°C/min.

from a ternary mixture of egg phosphatidylcholine, egg sphingomyelin, and cholesterol in equimolar proportions during a heating scan from 20 to 50°C. Phase separation is evident, particularly from the second-order lamellar reflection. The lamellar phase, which remains constant throughout the scan is ascribed to a cholesterol-rich phase that is in a liquid-ordered (Lo) configuration and corresponds in temperature independence to a binary mixture of sphingomyelin and cholesterol in equimolar proportions. The lamellar phase with a temperature-dependent *d*-spacing, by contrast, shows similar behavior to sphingomyelin containing lower proportions of cholesterol (shown in Fig. 5 *C*) and is presumed to be depleted of cholesterol relative to phospholipid. The separation illustrated by x-ray examination agrees with the data on ternary mixture comprising various SMs and phosphatidylcholines (in preparation). Differently, mixtures of oleoyl-SM, which is more easily miscible with PC do not separate in the presence of CHOL (Epand and Epand, 2004).

These data confirm that for sphingomyelin containing 33 mol% cholesterol there is no abrupt change in lamellar *d*-spacing but a continuous shift of the diffraction peak as a function of the temperature (Figs. 5 *C* and 6 *C*). For cholesterol concentrations of 41 and 50 mol% (Figs. 5 *D* and 6, *D–E*) there is also a single lamellar phase with a relatively temperature-independent behavior of both SAXS and WAXS peaks.

ESR

For all samples the spectra of the six ESR probes have been recorded at seven temperatures in the 17–53° range to determine S_{zz} and $\bar{\tau}$. Preliminary experiments were performed with a spin-probe concentration of 1 mol%. This concentration was subsequently reduced to 0.1 mol% to minimize the line broadening due to electron spin-spin interactions entailing large uncertainties in the determination of $\bar{\tau}$. On the other hand, the values found for S_{zz} were independent of the spin-probe concentration showing that it does not disturb the phase structure. The reduction of spin-spin interactions upon dilution shows that there is no segregation of the probe.

In pure egg sphingomyelin the transition between the weakly and strongly ordered Lα and Lβ phases appears as a marked increase of S_{zz} in a 10°C range centered about 35°C, which is progressively attenuated from PC-16 to PC-5 (data not shown). This Lα to Lβ transition is also clearly perceptible on the temperature dependence of $\bar{\tau}$ for PC-12, -14, and -16 probes (data not shown). For PC-5, PC-7, and PC-10 probes such discontinuity is less evident.

The temperature dependences of S_{zz} for PC-7 and PC-14 are shown as a function of CHOL concentration in Fig. 7. Only pure egg SM sample shows a break in the plot of S_{zz} versus temperature. For SM-CHOL samples the slope of the curves diminishes from SM-CHOL 17 mol% to SM-CHOL 41 mol%. Plots are flat for SM-CHOL 41 mol% and SM-CHOL 50 mol%. This parallels the evolution of the SAXS patterns (Fig. 6) and of the flattening of exotherms reported by differential scanning calorimetry (DSC) (Mannock et al., 2003) with cholesterol concentration. In particular the disappearance of the gel phase upon addition of only 17 mol% CHOL is confirmed. For clarity, the order parameters of Fig. 7 are given for a single site. For SM-CHOL 17 mol% and

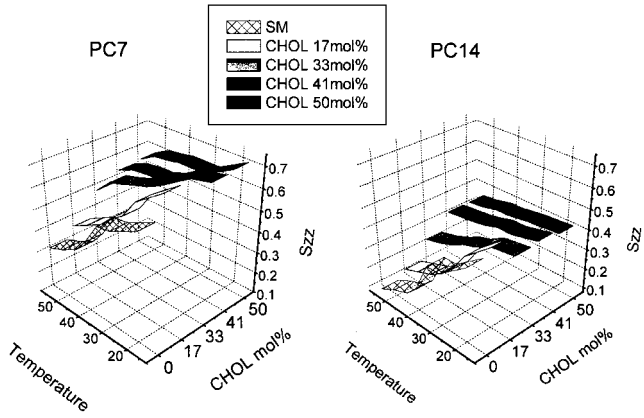

FIGURE 7 Dependence of the order parameters on temperature and cholesterol concentration for PC-7 and PC-14 spin probes. For clarity, the order parameter S_{ZZ} of the spin probes for SM-CHOL 17 mol% and SM-CHOL 33 mol% are given as the weighted average of S_{ZZ} values for sites A and B.

SM-CHOL 33 mol% mixtures where two sites have been evidenced, S_{zz} in Fig. 7 are the weighted average of the values obtained for these sites.

The ESR spectrum shown in Fig. 1 *B* is an example where the existence of two sites is perceptible by visual inspection. This is not always so easy. For example, we have verified, taking the order parameters of PC-5, 0.55 and 0.75, that an exchange rate as low as $5\times10^6\ s^{-1}$ is sufficient to erase any spectral feature revealing the existence of two sites. All spectra have, therefore, been systematically fitted on the assumptions of one and two sites using the LQCF or NLSL program. Using the LQCF program the fittings were also systematically performed with or without exchange between the sites. The discrimination between these different assumptions was based on the standard deviation values between the experimental and simulated spectra for PC-12, PC-14, and PC-16. For other doxyl positions the question of one or two sites cannot invariably be solved under the slow motional regime (below 40°C) where the spectral singularities of the two components are broad.

The existence of two sites denoted A and B, A being the most ordered, has been evidenced in samples containing CHOL 17 mol% and 33 mol%. For PC-12, PC-14, and PC-16, the spectral fittings are clearly improved introducing the exchange rate (ν_{ex}) between the sites as an additional adjustable parameter. Fig. 8 shows an example for an ESR spectrum where the existence of two sites is not evident at first sight except by a small bump indicated by an arrow at high field. Whereas the fitting for a single site seems already quite satisfactory, it is improved for two sites without exchange and is even better with $\nu_{ex} = 6\times10^6\ s^{-1}$. Spectral simulations show that the threshold for observing the two-sites exchange is $\nu_{ex} \approx 10^6\ s^{-1}$. The complete coalescence of the two components is achieved above $10^8\ s^{-1}$, ν_{ex} approaching the rates of reorientational and segmental motions. These limiting values depend on the proportion of the two sites and on the differences in the respective anisotropies of magnetic tensors. For SM-CHOL 17 mol% and SM-CHOL 33 mol% samples the intersite exchange rate ν_{ex} is found to vary between 1.5×10^6 and $10^7\ s^{-1}$ between 17 and 53°C (Fig. 9, *bottom*), a slow rate at the ESR timescale. The fractional population of site A (Fig. 9, *top*) shows a decay on heating the mixtures containing 17 and 33 mol% CHOL, a variation expected for the exothermic association between saturated phospholipids and cholesterol leading to the formation of condensed complexes (McConnell and Vrljic, 2003).

It is seen on Fig. 10 that for mixtures containing 17 mol% CHOL the temperature dependence of order parameters for PC-14 and PC-16 have parallel evolutions whereas slight deviations are observed between the values for SM-CHOL 33 mol%. The reorientation correlation time $\bar{\tau}$ is significantly shorter in site A than in site B, the difference diminishing as the temperature decreases until the two sites cannot be distinguished (Table 1). On the other hand, the spectra of

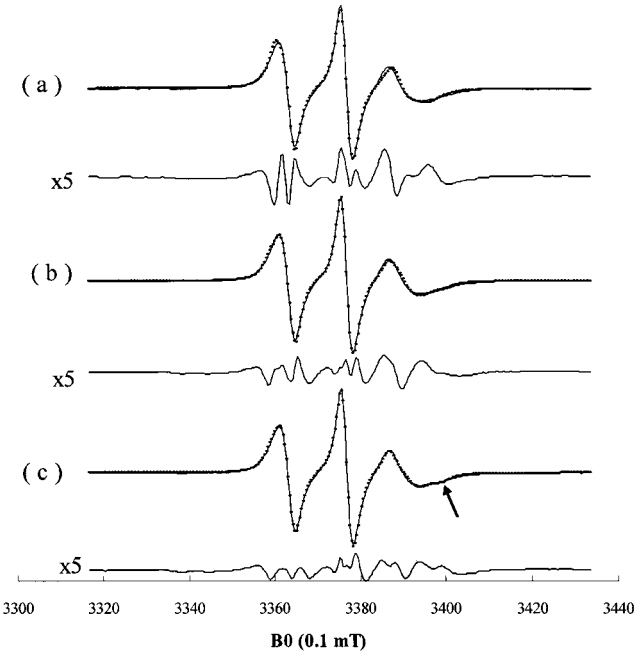

FIGURE 8 Experimental spectra (*solid line*), simulated spectra (*dots*), and difference spectra amplified five times (×5) of PC-14 spin probe in SM-CHOL 17 mol% at 37°C. The arrow denotes a feature suggesting the existence of two sites. The fittings yield the following parameters: (*a*) assuming a single site, $S_{zz} = 0.21$, $\bar{\tau} = 0.95$ ns; (*b*) assuming two sites and no intersite-exchange, fraction site A 0.34; site A, $S_{zz} = 0.33$, $\bar{\tau} = 0.59$ ns; site B, $S_{zz} = 0.14$, $\bar{\tau} = 1.0$ ns; (*c*) assuming two sites and intersite-exchange, fraction site A 0.52, exchange rate A↔B $\nu_{ex} = 6\times10^6\ s^{-1}$; site A, $S_{zz} = 0.36$, $\bar{\tau} = 0.45$ ns; site B, $S_{zz} = 0.14$, $\bar{\tau} = 1.2$ ns. The standard deviations between the experimental and computed spectra are (*a*) $\sigma = 1\%$, (*b*) $\sigma = 0.65\%$, (*c*) $\sigma = 0.35\%$.

spin probes in SM, SM-CHOL 41 mol%, and SM-CHOL 50 mol% samples are consistent with the existence of a single component in the whole temperature range investigated. The temperature dependence of ESR parameters of the Lo phase in the mixture containing 41 mol% CHOL characterized by x-ray diffraction is presented in Table 2 and shows a mono-exponential variation of $\bar{\tau}$ on $1/T$ and a high molecular order with a low-temperature dependence of S_{zz}. Essentially the same results are obtained with the SM-CHOL 50 mol% sample.

The most detailed information on the conformation and dynamics of the spin-labeled PC is achieved by taking into account the chain segmental motions by means of the DOXFIT program. The spectral fittings by this program have been limited to the 41–53°C range (Table 3) where the motions of reporter groups are under the fast motional regime or do not greatly exceed its limit. It is seen in Table 3 that addition of CHOL to SM reduces on the average $\tau_\perp^M$ by some 25% without any noticeable effect on the ratio $\rho = \tau_\perp^M/\tau_\parallel^M$. For all samples examined here, the overall reorientation is highly anisotropic with $\rho \approx 5$–6, greater than expected from the molecular dimensions of the phospholipids assimilated to an ellipsoid of longitudinal and equatorial

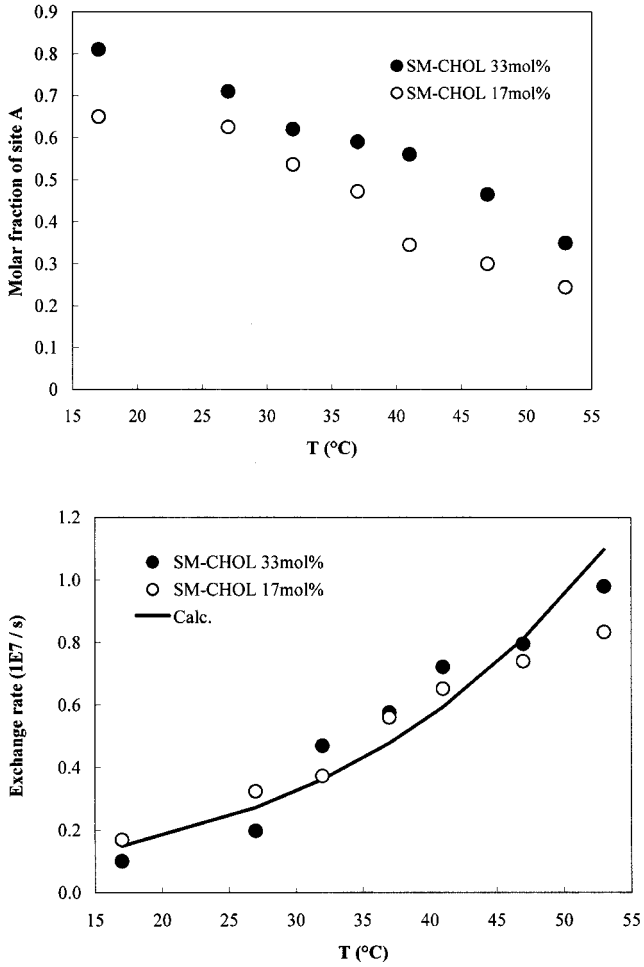

FIGURE 9 (*Top panel*) Fractional population of the most ordered site A for SM-CHOL 17 mol% (○) and SM-CHOL 33 mol% (●) calculated from the fittings of PC-12, PC-14, and PC-16 ESR spectra. (*Bottom panel*) Exchange rate between the sites A and B calculated from the spectral fittings for mixtures comprising SM-CHOL 17 mol% (○) and SM-CHOL 33 mol% (●). The solid line represents the least-squares fit for an exponential dependence of ν_{ex} on $1/T$ yielding $\nu_{ex}^{37^\circ} = 4.8\times10^6\ s^{-1}$ and an activation energy of 43 kJ/mol. From the diagram it is estimated that the lifetime of site A between 17 and 53°C varies from 0.44 to 0.02 μs and from 0.54 to 0.03 μs for CHOL 17 mol% and CHOL 33 mol%, respectively.

semiaxes 1.05 and 0.4 nm (Khelashvili and Scott, 2004) where ρ can be estimated to 2.63 using the expressions given in Tao (1969). This anisotropy is likely to result from the confinement of the spin probe and/or from an anisotropic viscosity of the medium with for example $\eta_{\|} = 6$ cP and $\eta_{\perp} = 14$ cP for pure SM at 41°C. The anisotropy of the overall motion has an increasing influence on linewidths as the position of the doxyl group becomes more distant from the polar head of the phospholipid because the z axis of magnetic tensors is, on average, less and less aligned with the longitudinal molecular axis Δ_M.

The rate of segmental motions is nearly independent of the presence of CHOL (Table 3), which enhances the population P_T of the *trans* rotamer about the C-C bonds, a well-known effect (see, for instance, Hubbell and McConnell, 1971) that is presently perceptible up to bonds 10–13 (Table 3). As a consequence of intermolecular constraints implicitly taken into account in the determination of P_T, the *trans* populations are found in the 0.80–0.95 range, well above the value of 0.5–0.6 for an unconstrained hydrocarbon chain in the same temperature range. Comparison of ESR and NMR data shows that the presence of the doxyl group has practically no influence on the molecular order parameter S_{mol} but modifies somewhat the intramolecular order parameter S_C (Moser et al., 1989). Moreover, the presence of this bulky group most likely inhibits the formation of complexes of spin-labeled PCs with cholesterol (Ahmed et al., 1997). The spin probes do not probably adopt the same conformations as the sphingomyelin molecules but reflect the local fluidity and chain flexibility in the membrane bilayers.

Small differences between the values given for P_T in Table 3 have a considerable impact on S_{zz} owing to their effects cumulated along the alkyl chain. A major influence of CHOL is to restrict the cross-sectional area available for the overall motion of the phospholipids (Mannock et al., 2003) with the exception of the polar head where this area is expanded by the presence of cholesterol (Guo et al., 2002). The influence of CHOL is observed on the molecular order parameter S_{mol} that exceeds 0.8 against 0.6–0.7 for pure SM. It may also be pointed out in Table 3 that for the site A of the SM-CHOL 17 mol% mixture, S_{mol} and P_T are close to the values obtained for the CHOL 41 and 50 mol% samples (Lo phase). For the site B, these parameters are significantly smaller than in the absence of CHOL when the spin probe is surrounded by the Lα phase formed by pure SM. The distinction between A and B sites provides additional evidence supporting the contention that the spin probes are not excluded from the ordered domains and segregated only into the disordered domains.

It seems likely that the A site corresponds to SM-CHOL condensed complexes whereas the B site is a disordered environment that does not undergo a transition with temperature. Indeed, no thermotropic transition is detected for SM-CHOL 17 mol% (Figs. 6 and 7). A sample of CHOL concentration of 17 mol% behaves similarly as a mixture containing 15 mol% assessed by ^{1}H magic angle spinning (MAS) NMR experiments at 25°C indicating an absence of Lβ pure SM clusters (Guo et al., 2002). This is also confirmed by ^{31}P NMR (Aussenac et al., 2003).

There is no straightforward relationship between the reorientation correlation time $\bar{\tau}$ obtained from LQCF or NLSL programs (Table 1) that treat S_{zz} as a global order parameter depending only on the doxyl position relative to the lipid/water interface and the dynamic parameters provided by the DOXFIT program (Table 3) where the molecular and segmental order parameters have distinct influences. The correlation times intervening in DOXFIT depend explicitly on the rates of segmental motions. Nevertheless $\bar{\tau}$ estimated by LQCF or NLSL (Table 1) is

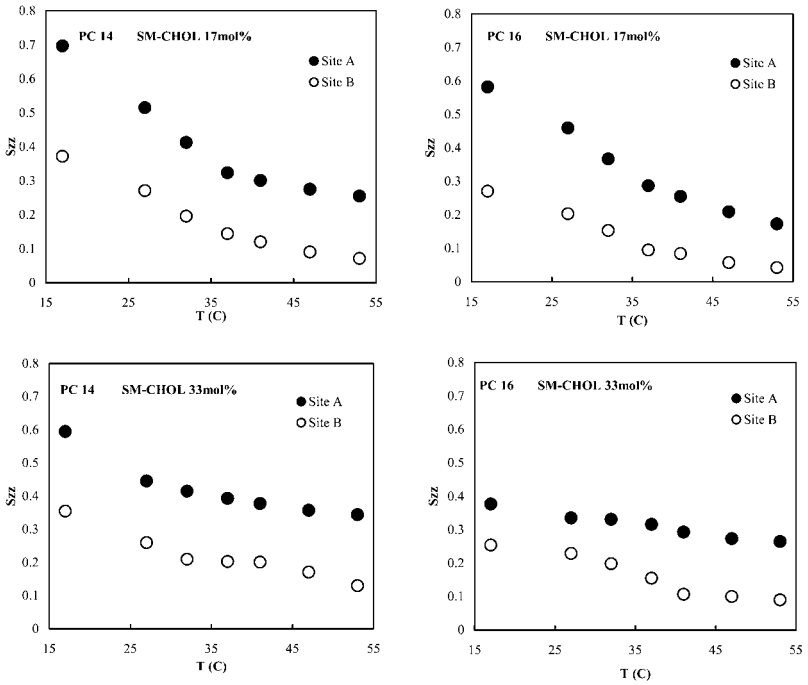

FIGURE 10 Temperature dependence of S_{zz} for PC-14 and PC-16 spin probe in site A (most ordered site, ●) and B (○) of SM-CHOL 17 mol% (*left panels*) and SM-CHOL 33 mol% (*right panels*).

a valuable indicator of the overall motion of doxyl groups according to the position in the chain and therefore an index of the fluidity of bilayers at different depths. The determination of $\bar{\tau}$ is closely related to the distinction pointed out by McConnell (1976) between S_{zz}^{obs} given by the reduced anisotropy of the hyperfine coupling $(a_{\parallel} - a_{\perp})/\ (a_{zz} - (1/2)(a_{xx} + a_{yy}))$ and the ''true'' order parameter S_{zz} (see also Fig. 1 in Wolf and Chachaty, 2000). S_{zz}^{obs} and S_{zz} diverge under the slow motional regime. If $\bar{\tau} > 2\ ns$, as it is often the case for PC-5 and PC-7 probes, S_{zz}^{obs} and the total spectral width 2 A_{max} depend simultaneously on both $\bar{\tau}$ and S_{zz}, making questionable the crude interpretations of ESR data using only 2 A_{max}, which do not discriminate motional effects from ordering effects for the highly viscous binary mixture formed by disaturated phospholipids and CHOL.

DISCUSSION

The manner in which domains of liquid-ordered phase are created in biological membranes and their size is currently of great interest in the context of the membrane raft hypothesis. This study addresses this question in a model system consisting of a binary mixture of sphingomyelin of natural origin and cholesterol. Two complementary biophysical methods that provide static structural information and dynamic spectroscopic parameters have been used.

Plasma membranes contain the building blocks for the creation of the Lo phase in the form of long-chain, high melting molecular species of sphingomyelin and cholesterol but the complexes do not appear to phase separate to form extensive domains in the membrane. The reason why such long-range phase separations do not occur could be due to the inherent mechanism of creation of the Lo phase and/or the dynamic nature of the processes of lipid phase separation in a system that is likely to be far from equilibrium. In this study it is assumed that the system is close to equilibrium so information fundamental to the creation of the Lo phase is obtained. The ESR results show that complexes between sphingomyelin and cholesterol are formed in the presence of a disordered phase of phospholipid when the proportion of cholesterol in the mixture is relatively low but creation of phase-separated domains of Lo structure has not been detected by synchrotron x-ray diffraction methods. With binary mixtures of these proportions (SM-CHOL 17 and 33 mol%) we found that:

1. The interdigitated phase of sphingomyelin is eliminated.
2. The temperature range over which the lamellar liquid-crystal repeat distance varies is considerably extended compared with bilayers of the pure phospholipid. The onset temperature during heating scans decreases from ~36 to 26°C in the presence of 17 mol% cholesterol. One possible interpretation for this broadening and consistent with 1 is that cholesterol preferentially associates with high melting molecular components of SM. Their very-long-chain species (C22, C24) are thought to form L_{β}* and bind CHOL with the highest affinity.
3. The disappearance of any gel phase characterized by sharp Bragg reflections in the WAXS region from mixtures containing 17 mol% cholesterol. This low concentration is able to inhibit the formation of gel clusters from the much more abundant SM as it was previously shown by NMR (Guo et al., 2002).

TABLE 1 Temperature dependence of the reorientation correlation time $\bar{\tau}$ versus temperature

		Cholesterol mol%					
	T (°C)	0%	17%*		33%*	41%	50%
PC-5	17	6.40	7.30		8.20	6.90	7.00
	27	4.00	5.20		6.10	5.40	5.40
	37	2.30	2.70		4.10	4.30	4.20
	47	1.70	1.30		1.87	3.50	2.80
PC-7	17	4.10	4.80		6.00	6.50	7.80
	27	2.40	3.40		5.90	5.00	4.80
	37	1.90	2.20		4.10	4.40	3.20
	47	1.70	1.20		2.80	2.80	1.50
			Site A	Site B			
PC-10	17	3.10	3.60	3.60	3.90	5.30	4.30
	27	2.25	2.80	2.65	2.80	3.90	3.00
	37	1.60	1.20	1.95	2.40	2.70	2.20
	47	1.40	0.55	1.00	1.80	2.00	1.70
					Site A	Site B	
PC-12	17	2.70	2.50	2.40	1.50	4.70	4.10	3.70
	27	2.25	1.20	2.30	1.10	3.40	2.30	2.50
	37	1.10	0.66	1.80	0.94	2.60	1.70	1.80
	47	0.80	0.34	1.00	0.45	2.20	1.20	1.00
PC-14	17	2.40	1.90	3.00	1.00	3.00	2.10	2.30
	27	2.30	1.30	2.10	0.85	2.70	1.20	1.40
	37	0.77	0.45	1.20	0.45	2.60	0.85	0.76
	47	0.57	0.31	0.90	0.37	2.20	0.57	0.56
PC-16	17	2.20	1.60	2.10	0.48	1.90	0.75	0.68
	27	1.40	1.20	1.60	0.36	1.50	0.55	0.41
	37	0.60	0.24	0.97	0.10	1.20	0.30	0.35
	47	0.40	0.15	0.83	0.06	1.00	0.26	0.38

*For SM-CHOL 17 and 33 mol% samples it happens that the values of $\bar{\tau}$ for sites A and B converge about nearly the same values or that their individual determination is unreliable. In this case their mean value or the value determined for a single site are given as reported in section Results.

4. ESR reveals two distinct environments probed by the spin-labeled PCs, the more ordered of the two displaying the characteristics expected for SM-CHOL complexes, namely, a high molecular order and a chain stiffening. The contribution of this ordered component to ESR spectra increases with the CHOL concentration until a single component signal is observed for SM-CHOL 41 mol%. However, SAXS shows a single lamellar phase for all CHOL concentrations investigated in the binary SM-CHOL mixture. In the lamellar phase observed with XRD, the *d*-spacing changes from a high-temperature dependence with mixtures containing 17 mol% cholesterol to invariance at CHOL 41 and 50 mol%.

TABLE 2 Order parameter S_{zz} and reorientation correlation time $\bar{\tau}$ of spin probes in the SM-CHOL 41 mol% sample

	E (kJ/ mol)	$\bar{\tau}$ 37° (ns)	S_{zz} 17°	S_{zz} 37°	S_{zz} 47°
PC-5	26.7	4.3	0.74	0.65	0.64
PC-7	26.4	3.6	0.69	0.60	0.59
PC-10	27.1	2.6	0.54	0.50	0.47
PC-12	28.5	1.7	0.44	0.42	0.37
PC-14	29.9	0.85	0.42	0.37	0.35
PC-16	25.5	0.37	0.31	0.28	0.26

The binary mixture forms a homogeneous single phase with characteristics assigned to the liquid-ordered phase. Corresponding activation energy and preexponential factor obtained from the least-squares fit of the temperature dependence of reorientation correlation times using $\bar{\tau} = \bar{\tau}_{310K}\exp[(E/R)((1/T) - (1/310))]$.

TABLE 3 Parameters obtained by means of the DOXFIT program for the ESR spectral fitting of spin-labeled PC-*n* in SM-CHOL mixtures

CHOL	T		Populations of the *trans* rotamer				$W_{G\to T}$	$\tau_\perp^M$	$\tau_\parallel^M$
(mol%)	(°C)	S_{mol}	Bonds n°:				($10^{10}s^{-1}$)	(ns)	(ns)
			1–6	7–9	10 and 11	12 and 13			
0%	41	0.72	0.93	0.91	0.90	0.88	0.7	4.5	0.75
	47	0.66	0.92	0.90	0.88	0.88	0.7	4.0	0.67
	53	0.62	0.91	0.89	0.81	0.78	1.0	3.6	0.57
17%	41	0.82	0.94	0.93	0.92	0.92	0.7	3.0	0.50
Site A	47	0.81	0.93	0.93	0.92	0.91	1.0	2.5	0.42
	53	0.78	0.93	0.92	0.91	0.90	1.2	2.0	0.33
17%	41	0.50	0.91	0.90	0.87	0.85	0.5	4.5	0.90
Site B	47	0.48	0.90	0.88	0.87	0.85	0.7	4.3	0.72
	53	0.46	0.88	0.87	0.85	0.83	1.0	3.3	0.55
41%	41	0.90	0.96	0.94	0.92	0.92	0.7	3.5	0.58
	47	0.86	0.95	0.94	0.92	0.92	1.0	3.0	0.60
	53	0.82	0.94	0.94	0.92	0.92	1.0	3.0	0.50
50%	41	0.89	0.96	0.95	0.93	0.93	0.6	4.0	0.67
	47	0.88	0.95	0.94	0.93	0.92	1.0	3.5	0.50
	53	0.84	0.94	0.94	0.93	0.92	1.0	3.0	0.38

S_{mol} is the molecular order parameter, i.e., the order parameter of the longitudinal axis Δ_M of the rotational diffusion tensor. $\tau_\perp^M$ and $\tau_\parallel^M$ are the correlation times for the tumbling motion of this axis and for the rotation about it. The population, P_T, of the *trans* rotamers about 13 C-C bonds of the *sn*-2 chain has been divided into four parts of equal probabilities. $W_{G\to T}$ is the probability per unit time of the *gauche* → *trans* transition. $W_{T\to G} = W_{G\to T}(1 - P_T)/2P_T$ and $W_{G^+\leftrightarrow G^-}$ are not given in the table. $W_{G^+\leftrightarrow G^-}$ is fixed to $0.05W_{G\to T}$ because the potential barrier between the two *gauche* is higher by 30–40 kJ/mol than between the *trans* and *gauche* rotamers (Flory, 1969) and has a very minor influence on the relaxation rates (Yasukawa and Chachaty, 1976). For most of the fittings, the angle between the axis Δ_M and Δ_C (mean axis of the *sn*-2 chain) is optimized to $\delta = 10°$ ($S_{tilt} = 0.955$).

At low CHOL concentrations, besides the ordered environment, ESR reveals a site that is even less ordered than the environment formed by pure SM above the transition temperature (Lα). This suggests that domains may be created that are too small to be organized into extended domains of Lα phase formed by SM in the absence of CHOL. Another possibility is that CHOL if not complexed with SM has a disordering effect. Aussenac et al. (2003) pointed out the very high ordering of CHOL in brain SM-CHOL 33 mol% ($S_{mol} \approx 0.9 - 1$). If the egg SM behaves as the brain SM, this suggests that most of CHOL molecules are located in the well-ordered site A.

The results indicate that there is no critical temperature and no threshold concentration of CHOL for the formation of a homogeneous Lo phase in binary mixtures formed with SM

of biological origin. This observation might be tentatively related to the variety of molecular species in natural lipids with different affinity for CHOL. Therefore, we assume that the creation of the Lo phase takes place by a gradual enrichment of the binary mixture in SM-CHOL condensed complexes without any long-range arrangement detectable by x-ray diffraction methods. This assumption implies that creation of Lo domains proceeds by a multiplication of ordered nanodomains rather than by their lateral extension. The possible reasons why SM-CHOL complexes do not form a separate Lo phase via a lateral diffusion of preexisting building blocks can be understood from the detailed analysis of the ESR spectra.

The two-sites exchange evidenced by ESR may correspond either to a lateral diffusion of the probe between two adjacent stable sites (model a), or to the limited lifetime of metastable sites where the probe is located (model b). In favor of model b, XRD shows a single phase. Using the same experimental setup SAXS detects multiple phase separation in tertiary (Fig. 5 *E*) and quaternary mixtures (Wolf et al., 2001). Another important argument that supports model b is the very short distance covered by the spin probe during the two-site exchange. Pulsed field gradient spin-echo NMR shows that between 40 and 60°C, the lateral diffusion coefficient D_L increases from $\sim 10^{-12}\,m^2s^{-1}$ to $7\times10^{-12}\,m^2s^{-1}$ in SM-CHOL mixtures containing 20% or more CHOL (Filippov et al., 2003). Extrapolating these data between 17 and 53°C yields a variation of D_L from $1.5\times10^{-13}\,m^2s^{-1}$ to $4\times10^{-12}\,m^2s^{-1}$. In this temperature range ESR measurements of the two-sites exchange rate gives a mean residence time of the probe in the ordered and disordered sites (model a) or a mean lifetime of these sites (model b), $\tau_s = 1/2\nu_{ex}$. Assuming that the diffusion coefficient of a spin-labeled PC in a membrane bilayer is similar to the surrounding phospholipid molecules one can estimate the root mean-square displacement $\bar{r}$ of a SM molecule during the exchange time of the ESR probe, $\tau_{ex} = \nu_{ex}^{-1}$. Taking $\tau_{ex} = 0.2\ \mu s$ and $D_L = 10^{-12}\,m^2s^{-1}$ at 37°C, one finds $\bar{r} = 2\sqrt{D_L\tau_{ex}} = 0.9\,nm$, a distance representing about one SM molecular diameter. As it cannot be ascertained that D_L is similar for PC spin probes and SM molecules, we have checked the estimate taking also the value $D_L = 2.25\times10^{-11}\,m^2s^{-1}$ determined for PC-16 in dimiristoylphosphatidylcholine (DMPC) bilayers at 37° (Sachse et al., 1987). The calculation yields $\bar{r} = 4\,nm$ for these SM-CHOL binary mixtures. The latter diffusion coefficient is also in reasonable agreement with the value $D_L = 1.5\times10^{-11}\,m^2s^{-1}$ obtained for DMPC molecules under similar conditions (Filippov et al., 2003) suggesting that there is no large difference between the diffusion coefficients of spin-labeled PC and SM molecules.

On the other hand, the assumption of a fast exchange on the ESR timescale (Sankaram and Thompson, 1990) is not consistent with the coexistence of Lα and Lo phases in the phase diagram assumed for SM-CHOL mixtures. The diffusion coefficients indicated above leads to extremely small domain dimensions ($0.15 < \bar{r} < 0.7\,nm$) and to τ_{ex} of a few nanoseconds, comparable to the tumbling correlation time $\tau_\perp^M$ of the spin probe.

The slow exchange observed presently at the ESR timescale is fast relative to exchange at the NMR timescale. The influence of exchange on NMR spectra depends on the anisotropies $\Delta\nu_{max}$ of the dipolar, quadrupolar, and chemical shielding tensors. For instance, in the case of phospholipids for $S_{zz} = 1$, the anisotropies of the ^{31}P (phosphate) and ^{13}C (carbonyl) shielding tensors at very high magnetic field (e.g., 11.75 Tesla) are 24 and 13 kHz, respectively, and the ^2H quadrupolar splittings in a methylene group is 280 kHz against 75–80 MHz for a nitroxide radical. If an exchange occurs between two sites A and B of order parameters S_{zz}^A and S_{zz}^B, the exchange timescale is formally $\tau_{ex} = (\Delta\nu_{max}|S_{zz}^A - S_{zz}^B|)^{-1}$ but τ_{ex} is measurable for much slower exchanges. The NMR measurement allows evaluation of the distance between sites separated by tens or hundreds of nanometers depending on the diffusion coefficient of the lipids. Thus, Huang et al. (1993) obtained from the ^{13}C chemical shift anisotropy $\tau_{ex} = 2\,ms$ in the case of dipalmitoyl- and distearoyl-phosphatidylcholine-CHOL 30 mol% mixture at 30°C. Taking $D_L = 2\times10^{-12}\,m^2s^{-1}$ (Vist and Davis, 1990) instead of the value of $10^{-14}\,m^2s^{-1}$ possibly underestimated by two or more orders of magnitude (Huang et al., 1993) the intersites distance is estimated to 130 nm, a distance consistent with the phase separation. Others (Vist and Davis, 1990) have delineated the phase boundaries for DPPC-CHOL mixtures by difference NMR spectroscopy of ^2H superimposed spectra. They pointed out that this method, which assumes no exchange, does not hold above 38°C for CHOL 22.5–25 mol% where the exchange becomes fast at an exchange timescale of 75 μs. For $D_L = 2\times10^{-12}\,m^2s^{-1}$ they estimate $\bar{r} < 25\,nm$. The authors suggested that ESR would be more appropriate in this case to the evaluation of the intersites distance.

Under conditions comparable to this study, experiments such as ^1H, ^{13}C, ^{31}P MAS-NMR, and ^2H-NMR (Guo et al., 2002), ^2H and ^{31}P-NMR (Aussenac et al., 2003) showed a single signal for each nucleus, which may be interpreted as the existence of one site. It may also be the result of a fast exchange among two or more sites. From MAS experiments on brain SM-CHOL mixtures, Guo et al. (2002) ascribed the variations of chemical shifts at increasing cholesterol concentrations to the successive existence of Lα, Lα + Lo and Lo phases. The data were in rough agreement with the phase diagram proposed by Sankaram and Thompson (1990). However, the coexistence of two phases in the intermediate region of this diagram is questionable because it is not supported by the measurements of the exchange times and lateral diffusion coefficients. Finally, NMR data can also be interpreted in terms of two sites formed by the ordered and disordered molecular clusters.

The study of Filippov et al. (2003) suggested that Arrhenius's plots of D_L are not linear at cholesterol concentrations lower than 30–40% as a consequence of the

heterogeneous composition of the natural phospholipid used for the measurements. As the lateral diffusion of SM molecules is slow compared to other phospholipids, it is possible that the different molecular species are not randomly distributed and form local aggregates of particular composition with different affinities for cholesterol. The interpretation of NMR data is therefore consistent with the present XRD and ESR study that does not show extended domain separation in the binary egg SM-CHOL 17% and 33% mixtures. This interpretation seems also consistent with DSC studies. Thermograms resolved by DSC in mixtures of DPPC-CHOL consist of a narrow and a broad peak at 16.5 and 19% CHOL, said to signify coexistence of two immiscible phases (Mabrey et al., 1978). With greater proportions of CHOL only the broad component remains. In the case of the egg SM-CHOL mixture on the contrary, there is no convincing evidence for the coexistence of two phases at 16% CHOL. At this concentration and above, wide structureless thermograms that broaden as the cholesterol concentration is augmented are observed up to 50 mol% CHOL (Mannock et al., 2003; Fig. 2 *A*).

Mixed with cholesterol egg sphingomyelin would progressively form an homogeneous Lo phase rather than separated poorly and highly ordered extended domains as it is observed for synthetic disaturated phospholipid mixtures. However, it cannot be assumed that the model proposed for egg sphingomyelin-cholesterol can be extended directly to other mixtures including biological phospholipids and cholesterol because the phase behavior depends also possibly on the variety of composition that influences affinity for CHOL and diffusion rates of the distinct species.

CONCLUSION

The timescale for the two-site exchange observed by ESR methods is much too short to be compatible with the diffusion of the spin probe between extended domains. It seems likely that the ESR spin probes are located in an environment comprising both short-lived SM-CHOL condensed complexes and disordered molecular clusters of the type shown schematically in Fig. 11. The dynamic equilibrium among these nanodomains results possibly from fluctuations in the local concentrations of cholesterol diffusing rapidly. However, no values are available on the cholesterol diffusion coefficient. At high concentrations of cholesterol the phase becomes saturated by condensed complexes thus eliminating all disordered clusters of phospholipid. This is the case for mixtures of sphingomyelin and cholesterol of 41 mol% or more where the temperature independence of the molecular ordering and the *d*-spacing are observed by ESR and x-ray diffraction methods, respectively.

The synchrotron x-ray diffraction measurements were ably assisted by Dr. Anthony Gleeson.

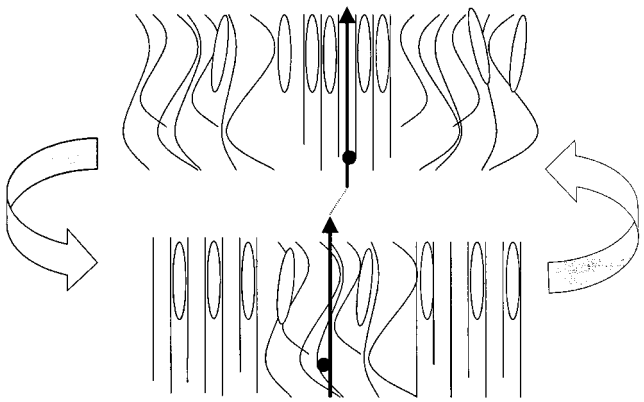

FIGURE 11 Model of a SM-CHOL leaflet containing the spin probe (*vertical arrow*). The stiff or curved lines represent SM and the ellipses CHOL. During its displacement (a few nanometers), the probe experiences successively highly ordered and poorly ordered environments due to the creation and disruption of short-life SM-CHOL condensed complexes.

REFERENCES

Ahmed, S. N., D. A. Brown, and E. London. 1997. On the origin of sphingolipid/cholesterol-rich detergent-insoluble cell membranes: physiological concentrations of cholesterol and sphingolipid induce formation of a detergent-insoluble, liquid-ordered lipid phase in model membranes. *Biochemistry.* 36:10944–10953.

Almeida, P. F., W. L. Vaz, and T. E. Thompson. 1992. Lateral diffusion in the liquid phases of dimyristoylphosphatidylcholine/cholesterol lipid bilayers: a free volume analysis. *Biochemistry.* 31:6739–6747.

Aussenac, F., M. Tavares, and E. J. Dufourc. 2003. Cholesterol dynamics in membranes of raft composition: a molecular point of view from 2H and 31P solid-state NMR. *Biochemistry.* 42:1383–1390.

Boggs, J. M., and K. M. Koshy. 1994. Do the long fatty acid chains of sphingolipids interdigitate across the center of a bilayer of shorter chain symmetric phospholipids? *Biochim. Biophys. Acta.* 1189:233–241.

Boulin, C., R. Kempf, A. Gabriel, M. Koch, and S. McLaughlin. 1986. Data appraisal, evaluation and display for synchrotron radiation experiments: hardware and software. *Nucl. Instrum. Methods.* 249:399–409.

Budil, D. E., S. Lee, S. Saxena, and J. H. Freed. 1996. Non-linear least squares analysis of slow motion EPR spectra in one and two dimensions using a modified Levenberg-Marquardt algorithm. *J. Magn. Reson. Ser. A.* 120:155–189.

Calhoun, W. I., and G. G. Shipley. 1979. Sphingomyelin-lecithin bilayers and their interaction with cholesterol. *Biochemistry.* 18:1717–1722.

Caniparoli, J. P., A. Grassi, and C. Chachaty. 1988. Correlated internal motions and nuclear spin relaxation in lamellar mesophases. *Mol. Phys.* 63:419–431.

Cassol, R., A. Ferrarini, and P. L. Nordio. 1993. Dynamics of nitroxide probes linked to flexible chains. *J. Phys. Chem.* 97:2933–2940.

Cassol, R., M. Ge, A. Ferrarini, and J. H. Freed. 1997. Chain dynamics and the simulation of electron spin resonance spectra from oriented phospholipid membranes. *J. Phys. Chem. B.* 101:8782–8789.

Chachaty, C., and T. Bredel. 1991. Surfactant-counterion dynamics in pyridinium octyl phosphate lyotropic mesophases. A nuclear relaxation study. *J. Phys. Chem.* 95:5335–5344.

Chachaty, C., and G. Langlet. 1985. Logiciels d'étude conformationnelle de molécules flexibles. *J. Chim. Phys.* [in French]. 82:614–619.

Chachaty, C., and E. Soulié. 1995. Determination of ESR static and dynamic parameters by automated fitting of spectra. *J. Phys. III France.* 5:1927–1952.

Chachaty, C., and C. Wolf. 1999. An application of ESR spectral simulation methods to doxylstearic spin probes in pure and mixed sphingomyelin bilayers. Effect of sterol additives. *Molecular Physics Reports.* 26:143–150.

Davoust, J., and P. F. Devaux. 1982. Simulation of electron spin resonance spectra of spin-labeled fatty acids covalently attached to the boundary of an intrinsic membrane protein. A chemical exchange model. *J. Magn. Reson.* 48:475–494.

Dietrich, C., L. A. Bagatolli, Z. N. Volovyk, N. L. Thompson, M. Levi, K. Jacobson, and E. Gratton. 2001. Lipid rafts reconstituted in model membranes. *Biophys. J.* 80:1417–1428.

Edidin, M. 2003. The state of lipid rafts: from model membranes to cells. *Annu. Rev. Biophys. Biomol. Struct.* 32:257–283.

Epand, R. M., and R. F. Epand. 2004. Non-raft forming sphingomyelin-cholesterol mixtures. *Chem. Phys. Lipids.* 132:37–46.

Filippov, A., G. Oradd, and G. Lindblom. 2003. The effect of cholesterol on the lateral diffusion of phospholipids in oriented bilayers. *Biophys. J.* 84:3079–3086.

Flory, P. J. 1969. Conformational energies of n-alkanes. *In* Statistical Mechanics of Chain Molecules. Wiley Interscience, New York, NY. 133–140.

Freed, J. H. 1977. Stochastic molecular theory of spin relaxation for liquid crystals. *J. Chem. Phys.* 66:4183–4199.

Gandhavadi, M., D. Allende, A. Vidal, S. A. Simon, and T. J. McIntosh. 2002. Structure, composition, and peptide binding properties of detergent soluble bilayers and detergent resistant rafts. *Biophys. J.* 82:1469–1482.

Ge, M., K. A. Field, R. Aneja, D. Holowka, B. Baird, and J. H. Freed. 1999. Electron spin resonance characterization of liquid ordered phase of detergent-resistant membranes from RBL-2H3 cells. *Biophys. J.* 77:925–933.

Guo, W., V. Kurze, T. Huber, N. H. Afdhal, K. Beyer, and J. A. Hamilton. 2002. A solid-state NMR study of phospholipid-cholesterol interactions: sphingomyelin-cholesterol binary systems. *Biophys. J.* 83:1465–1478.

Hagen, J. P., and H. M. McConnell. 1997. Liquid-liquid immiscibility in lipid monolayers. *Biochim. Biophys. Acta.* 1329:7–11.

Huang, T. H., C. W. Lee, S. K. Das Gupta, A. Blume, and R. G. Griffin. 1993. A 13C and 2H nuclear magnetic resonance study of phosphatidylcholine/cholesterol interactions: characterization of liquid-gel phases. *Biochemistry.* 32:13277–13287.

Hubbell, W. L., and H. M. McConnell. 1971. Molecular motion in spin-labeled phospholipids and membranes. *J. Am. Chem. Soc.* 93:314–326.

Ipsen, J. H., G. Karlstrom, O. G. Mouritsen, H. Wennerstrom, and M. J. Zuckermann. 1987. Phase equilibria in the phosphatidylcholine-cholesterol system. *Biochim. Biophys. Acta.* 905:162–172.

Khelashvili, G. A., and H. L. Scott. 2004. Combined Monte Carlo and molecular dynamics simulation of hydrated 18:0 sphingomyelin-cholesterol lipid bilayers. *J. Chem. Phys.* 120:9841–9847.

Koumanov, K. S., C. Tessier, A. B. Momchilova, D. Rainteau, C. Wolf, and P. J. Quinn. 2005. Comparative lipid analysis and structure of detergent-resistant membrane raft fractions isolated from human and ruminant erythrocytes. *Arch. Biochem. Biophys.* 434:150–158.

Kurad, D., G. Jeschke, and D. Marsh. 2004. Lateral ordering of lipid chains in cholesterol-containing membranes: high-field spin-label EPR. *Biophys. J.* 86:264–271.

Lange, A., D. Marsh, K. H. Wassmer, P. Meier, and G. Kothe. 1985. Electron spin resonance study of phospholipid membranes employing a comprehensive line-shape model. *Biochemistry.* 24:4383–4392.

Livshits, V., D. Kurad, and D. Marsh. 2004. Simulation studies on high-field EPR spectra of lipid spin labels in cholesterol-containing membranes. *J. Phys. Chem. B.* 84:1038–1046.

Lou, Y., M. Ge, and J. H. Freed. 2001. A multifrequency ESR study of the complex dynamics of membranes. *J. Phys. Chem.* 105:11053–11056.

Mabrey, S., P. L. Mateo, and J. M. Sturtevant. 1978. High-sensitivity scanning calorimetric study of mixtures of cholesterol with dimyristoyl- and dipalmitoylphosphatidylcholines. *Biochemistry.* 17:2464–2468.

Mannock, D. A., T. J. McIntosh, X. Jiang, D. F. Covey, and R. N. McElhaney. 2003. Effects of natural and enantiomeric cholesterol on the thermotropic phase behavior and structure of egg sphingomyelin bilayer membranes. *Biophys. J.* 84:1038–1046.

Marquardt, D. W. 1963. An algorithm for least-squares estimation of nonlinear parameters. *J. Soc. Ind. Appl. Math.* 11:431–441.

Marsh, D. 1989. Experimental methods in spin-label spectral analysis and two-site exchange simulation. *In* Spin Labeling Theory and Applications: Biological Magnetic Resonance. L. J. Berliner and J. Reuben, editors. Plenum Press, New York, NY. 255–303.

McConnell, H. M. 1976. Molecular motion in biological membranes, Appendix A, rotational correlation times. *In* Spin Labeling Theory and Applications, Vol. I. L. Berliner, editor. Academic Press, New York, NY. 554–556.

McConnell, H. M., and M. Vrljic. 2003. Liquid-liquid immiscibility in membranes. *Annu. Rev. Biophys. Biomol. Struct.* 32:469–492.

Moser, M., D. Marsh, P. Meier, K. H. Wassmer, and G. Kothe. 1989. Chain configuration and flexibility gradient in phospholipid membranes. Comparison between spin-label electron spin resonance and deuteron nuclear magnetic resonance, and identification of new conformations. *Biophys. J.* 55:111–123.

Nordio, P. L. 1976. General magnetic resonance theory and linewidths parameters. *In* Spin Labeling Theory and Applications, Vol. 1. L. Berliner, editor. Academic Press, New York, NY. 1–52.

Recktenwald, D. J., and H. M. McConnell. 1981. Phase equilibria in binary mixtures of phosphatidylcholine and cholesterol. *Biochemistry.* 20:4505–4510.

Rinia, H. A., M. M. Snel, J. P. van der Eerden, and B. de Kruijff. 2001. Visualizing detergent resistant domains in model membranes with atomic force microscopy. *FEBS Lett.* 501:92–96.

Sachse, J., D. King, and D. Marsh. 1987. ESR determination of lipid translational diffusion coefficients at low spin-label concentrations in biological membranes using exchange broadening, exchange narrowing and dipole-dipole interactions. *J. Magn. Reson.* 71:385–404.

Sankaram, M. B., and T. E. Thompson. 1990. Interaction of cholesterol with various glycerophospholipids and sphingomyelin. *Biochemistry.* 29:10670–10675.

Schneider, D. J., and J. H. Freed. 1989. Calculating slow motional magnetic resonance spectra. A user's guide. *In* Spin Labeling Theory and Applications, Biological Magnetic Resonance. L. J. Berliner and J. Reuben, editors. Plenum Press, New York, NY. 1–76.

Tao, T. 1969. Time dependent fluorescence depolarization and Brownian rotational diffusion coefficients of macromolecules. *Biopolymers.* 8:600–632.

Vist, M. R., and J. H. Davis. 1990. Phase equilibria of cholesterol/dipalmitoylphosphatidylcholine mixtures: ^{2}H nuclear magnetic resonance and differential scanning calorimetry. *Biochemistry.* 29:451–464.

Wolf, C., and C. Chachaty. 2000. Compared effects of cholesterol and 7-dehydrocholesterol on sphingomyelin-glycerophospholipid bilayers studied by ESR. *Biophys. Chem.* 84:269–279.

Wolf, C., K. Koumanov, B. Tenchov, and P. J. Quinn. 2001. Cholesterol favors phase separation of sphingomyelin. *Biophys. Chem.* 89:163–172.

Yasukawa, T., and C. Chachaty. 1976. Steric effects on the dynamical behavior and nuclear spin relaxation in flexible molecules. *Chem. Phys. Lett.* 45:565–567.